

Phonons in colloidal crystals

R. S. PENCIU^{2(*)}, M. KAFESAKI¹, G. FYTAS^{1,3}, E. N. ECONOMOU^{1,2},
W. STEFFEN³, A. HOLLINGSWORTH⁴ and W. B. RUSSEL⁴

¹ *FORTH, Institute of Electronic Structure and Laser*

P.O. Box 1527, 71110 Heraklion, Crete, Greece

² *Physics Department, University of Crete - Heraklion, Greece*

³ *Max-Planck Institute for Polymer Research*

P.O. Box 3148, 55128 Mainz, Germany

⁴ *Department of Chemical Engineering, Princeton University*
Princeton, NY 08544, USA

(received 9 November 2001; accepted in final form 7 March 2002)

PACS. 63.20.-e – Phonons in crystal lattices.

PACS. 82.70.Dd – Colloids.

PACS. 62.30.+d – Mechanical and elastic waves; vibrations.

Abstract. – The dispersion curves of the phonons propagating in polycrystalline suspensions of hard-sphere colloids are measured by Brillouin scattering and calculated by band structure techniques. Acoustic-like and optical-like experimental phonon dispersion relations are attributed to the interplay of the solvent matrix mode with the single-sphere vibration eigenmodes in these lattice structures.

The propagation of acoustic waves through inhomogeneous media has long been a subject of interest since the spatial modulation in density and elastic parameters can give rise to fascinating rich behavior with practical relevance [1–3]. As more self-assembled mesoscopic structures emerge, long-wavelength elastic excitations can be probed by non-invasive Brillouin spectroscopy with direct access to the desired reciprocal space, since the typical size of an elementary cell is of the order of μm (in contrast to the conventional crystals of atomic dimensions, the phonon spectrum of which is well documented [4]). Lattice dynamics associated with the overdamped longitudinal and transverse acoustic branch in the first and second Brillouin zone [4] were recently studied in a single (volume fraction $\phi = 0.54$) hard-sphere [5] colloidal crystal and a dilute ($\phi = 0.003$) charged stabilized colloidal crystal [6], using quasi-elastic light scattering.

Employing inelastic light scattering, we present the first, to the best of our knowledge, experimental results on the frequencies and the dispersion relations of phonons propagating in two polycrystalline colloids consisting of: a) PMMA spheres of diameter $d \approx 605$ nm and $\phi \approx 0.52$ in an almost symmetric decalin/tetralin mixture and b) silica spheres of $d \approx 250$ nm

(*) Permanent address: National Institute for Research and Development in Materials Physics - Bucharest, Romania.

and volume fraction $\phi \approx 0.62$ in cyclohexane/decalin. Case b), in contrast to case a), involves large mismatch in the elastic constants and the densities between the spheres and the host medium [7]. We map out the observed phonon spectra (up to five modes) of these two colloidal polycrystals and compare the experimental to the calculated dispersion relations. Distinct differences between case a) and case b) appear, due to the hardness of the silica particles as opposed to the softness of the PMMA spheres.

The phonon propagation in the colloidal crystals was monitored by Brillouin light scattering spectroscopy in the GHz frequency range and for different qd values, between 0.97 and 21.8 approximately, where $q = |\mathbf{q}_i - \mathbf{q}_f| = (4\pi n/\lambda) \sin(\theta/2)$ (\mathbf{q}_i and \mathbf{q}_f are, respectively, the wave vector of the incident and the scattered light, λ ($= 514.5$ nm) is the wavelength of the laser, n is the refractive index of the medium and θ is the scattering angle). Polarized Brillouin spectra arising from thermal density fluctuations in the system were recorded [8] by a six-pass tandem-Fabry-Perot interferometer, using two free spectral ranges (7.5 GHz and 30 GHz) for each spectrum (in order to achieve both high-resolution and broad frequency range). In the homogeneous media that cannot support shear, *e.g.* the solvents, one Brillouin doublet $\pm\omega$ shifted about the Rayleigh line is observed due to the absorption or emission of one longitudinal phonon with phase velocity $c_l = \omega/q$. The present polycrystalline systems exhibit clear Bragg scattering; for PMMA it resembles that of fig. 1b in ref. [9]. Hence, the static structure factor peaks at $q^* = 0.0113$ nm $^{-1}$ for the PMMA and at $q^* = 0.029$ nm $^{-1}$ for the silica colloidal crystals. The size of the grains, as estimated from the width of these first-order peaks, is about $9d$ for PMMA and $15d$ for silica. The adequate orientational average of the phonon spectrum was proven by examining recorded Brillouin spectra for different cell orientations and positions; the probed volume has a diameter of ca. 150 μ m.

Figure 1 shows high-resolution Brillouin spectra for the PMMA crystal (case a)) at three scattering wave vectors, q . The spectra recorded at two free spectral ranges were spliced together using a constant intensity factor. Up to four (at highest q) Brillouin doublets are observed in this crystalline sample, in clear distinction to the Brillouin spectrum of the liquid suspension of PMMA spheres [10]. At a given q , the location of the peaks in the polarized Brillouin spectrum of fig. 1 defines the experimental phonon frequencies; the colloidal suspension displays a broad featureless Rayleigh-Brillouin spectrum in the depolarized geometry.

The inelastic light scattering cross-section, $d^2\sigma/d\Omega d\omega_f$, by a phonon of wave vector \mathbf{k} and branch s ($s = 1, 2, 3, \dots$) is given by

$$\frac{d^2\sigma}{d\Omega d\omega_f} \propto \frac{k_B T}{\omega_{\mathbf{k}s}^2} |A_{\mathbf{q}}|^2 [\delta(\omega - \omega_{\mathbf{k}s}) \delta_{\mathbf{q}, \mathbf{k} + \mathbf{K}_m} + \delta(\omega + \omega_{\mathbf{k}s}) \delta_{\mathbf{q}, -\mathbf{k} - \mathbf{K}_m}], \quad (1)$$

where $A_{\mathbf{q}} = \sum_{\mathbf{K}'_m} \nu_{\mathbf{K}'_m} (\mathbf{q} - \mathbf{K}'_m) \cdot \tilde{\mathbf{u}}_{\mathbf{q} - \mathbf{K}'_m}$; $\mathbf{K}_m, \mathbf{K}'_m$ are vectors of the reciprocal lattice, $\nu_{\mathbf{K}'_m}$ is the normalized Fourier coefficient of the electron concentration, $\tilde{\mathbf{u}}_{\mathbf{q} - \mathbf{K}'_m}$ is the normalized Fourier coefficient of the phonon displacement vector $\mathbf{u}_{\mathbf{k}s}(\mathbf{r})$, and $\omega \equiv \omega_i - \omega_f$. The momentum $\hbar\mathbf{q}$ lost by the photon is transferred in part to the phonon, $\hbar\mathbf{k}$, and in part to the periodic lattice, $\hbar\mathbf{K}_m$. It follows that the peak at $\omega = \omega_{\mathbf{k}s}$ may appear not only at $\mathbf{q} = \mathbf{k}$, as in a uniform medium, but at more than one $\mathbf{q} = \mathbf{k} + \mathbf{K}_m$, depending on the magnitude of $|A_{\mathbf{q}}|^2$. For acoustic branches, where $\omega_{\mathbf{k}s} \sim k$ ($k = |\mathbf{k}|$), and for $kd \ll 1$, the sum in $A_{\mathbf{q}}$ is dominated by the term $\tilde{\mathbf{u}}_{\mathbf{k}}$ and, consequently, $A_{\mathbf{q}} \approx A_{\mathbf{k}} \approx \mathbf{k} \cdot \tilde{\mathbf{u}}_{\mathbf{k}}$.

In fig. 2 we plot for the case a) the experimental frequencies $\omega_{\mathbf{k}s}$ *vs.* qd , together with the results of theoretical calculations performed by employing established band structure techniques for solving the elastic wave equation which depends on the densities and the elastic constants; the interparticle potential plays a minor role in the phonon dispersion. We chose an infinite periodic fcc lattice taking into account that the structure is usually either hcp

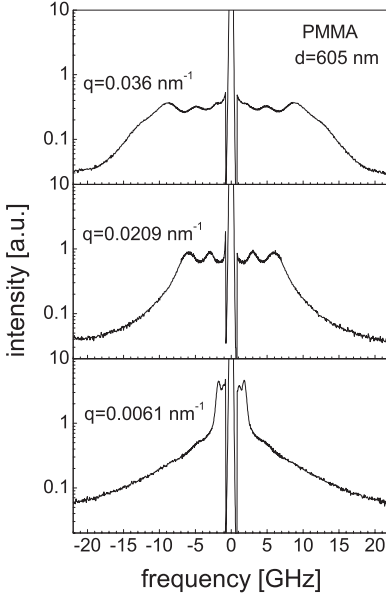


Fig. 1

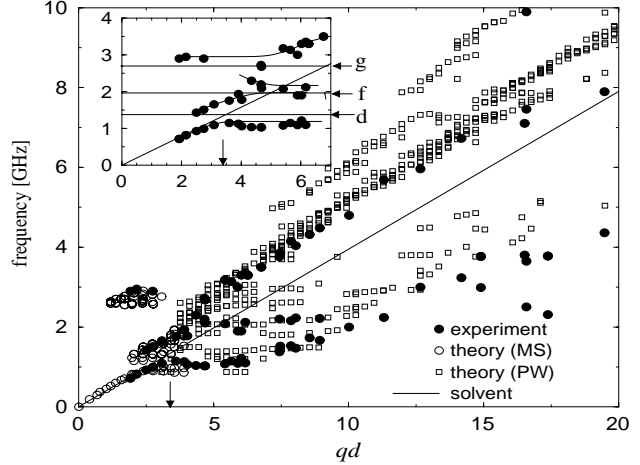


Fig. 2

Fig. 1 – Polarized Brillouin spectra obtained at three scattering wave vectors, q , for a colloidal crystal consisting of PMMA spheres (of diameter $d \approx 605$ nm and volume fraction $\phi \approx 0.52$) in an almost symmetric decalin/tetralin mixture, at 20 °C. The frequency region which lies approximately ± 0.5 GHz from the central peak is fed to the reference beam used for the stabilization of the interferometer.

Fig. 2 – Phonon dispersion relations for the system of fig. 1. Solid circles denote the experimental data. Open circles and open squares denote theoretical results based on the multiple scattering (MS) and the plane wave (PW) method, respectively. The experimental points for $qd < 7$ are replotted in the inset together with lines to guide the eye. The arrows on the vertical axis of the inset and the horizontal lines indicate the frequencies of the (slightly damped) eigenmodes of a single PMMA sphere embedded in the solvent; the letters next to them denote the spherical harmonic character of these eigenmodes. The arrow on the horizontal axis corresponds to the center-surface distance of the first Brillouin zone in the [111] direction. The solid line fits the measured dispersion relation for the longitudinal phonons in the solvent.

or fcc [5, 9], and that the latter facilitates the calculations without significantly affecting the theoretical results. The open circles represent phonon dispersion relations, $\omega_{\mathbf{k}s}$ vs. $|\mathbf{k} + \mathbf{K}_m|d$, obtained by a sophisticated multiple scattering (MS) method [11], which is very reliable for low frequencies but too costly to extend to higher values. To remedy this deficiency we also employed the plane wave (PW) method [4, 12] (open squares in fig. 2) which, in addition, allows a direct estimation of the amplitude $A_{\mathbf{q}}$; however, the PW method forces us to treat the solvent as artificially possessing a small shear modulus, G . We kept only those $\omega_{\mathbf{k}s}$ vs. \mathbf{k} points which do not change as G becomes smaller and smaller. There is a proliferation of theoretical points because for each calculated $(\mathbf{k}, \omega_{\mathbf{k}s})$ point (\mathbf{k} in the first Brillouin zone (BZ)) we created many equivalent points by adding various \mathbf{K}_m vectors to \mathbf{k} . This is necessary, since in a polycrystalline sample the vector \mathbf{K}_m , which reduces the measured momentum transfer, $\hbar\mathbf{q}$, to the first BZ, cannot be obtained experimentally. In fig. 2 we kept those theoretical points which correspond to phonons with strong coupling to the photons, *i.e.* large intensity in eq. (1).

To obtain a simple physical picture of the observed modes we also calculated the eigen-

modes [13] of a single PMMA sphere embedded in the decalin/tetralin solvent; these eigenmodes were obtained from the resonances in the scattering cross-section of a plane *acoustic* wave by a single PMMA sphere; the corresponding eigenfrequencies are indicated by arrows (in the frequency axis) and horizontal lines in the inset of fig. 2. The overall agreement between the theoretical results and the experimental data is good, given that no adjustable parameter was involved. The low- q acoustic mode is confined predominantly in the solvent as evident by the fact that the phase velocity, both experimentally and theoretically, almost coincides with the phase velocity of the solvent. Furthermore, as ω and q are increased ($\omega \lesssim 3$ GHz, $qd \lesssim 8$) the results can be interpreted, to a first approximation, as hybrids due to the coupling of the $\omega = c_1 k$ longitudinal solvent mode with the local modes of each individual PMMA sphere as shown by the crossovers in the inset of fig. 2. Since the contrast in the elastic constants and density between the solvent and the PMMA is rather low, this coupling is expected and found to be strong, leading to an acoustic gap. The latter is, probably, further enhanced because it almost coincides with the boundaries of the first BZ (arrow on the x -axis of fig. 2). The modes beyond the arrow correspond to $|\mathbf{q}| = |\mathbf{k} + \mathbf{K}_m|$ with $\mathbf{K}_m \neq 0$. Finally, the high- q -high- ω spectrum is dominated by an average acoustic-like mode shared by both components, as confirmed by explicit displacement field calculations. The high- q -low- ω modes are associated mostly with individual spheres. Both modes are present in the colloidal liquid phase [10], the main difference confined in the vicinity of the first Brillouin zone edges.

We present next (see fig. 3) the rich phonon spectrum of the silica colloidal crystal (case b)), where the elastic constants contrast [7] between the silica spheres and the solvent is large. Up to five hypersonic excitations at a given wave vector can be resolved, with quite different amplitudes in contrast to the phonons in fig. 1. In fig. 4 we display the experimental points $\omega_{\mathbf{k}s}$ vs. qd for the silica colloidal crystal, together with the theoretical results. The arrows in the vertical axis indicate theoretical results, obtained as in case a), for the eigenfrequencies of a single silica sphere embedded in cyclohexane/decalin. The open circles represent theoretical dispersion relations, $\omega_{\mathbf{k}s}$ vs. $|\mathbf{k} + \mathbf{K}_m|d$, obtained by the MS band structure method [11]. The lowest ($s = 1$) frequency branch, $\omega_{\mathbf{k}1}$ vs. qd , corresponds to an acoustic phonon, since its dispersion curve matches well the theoretical first band in the first Brillouin zone. Furthermore, comparing this dispersion curve at low q with that of the longitudinal phonon in the pure fluid (solid line in fig. 4), one can see that the corresponding velocity is slightly higher than that in the solvent. This indicates that the propagation takes place almost exclusively through the fluid with only a minute fraction in the silica spheres.

The dispersion curves of the next two branches ($s = 2, 3$) are in reasonable agreement with the corresponding theoretical bands, for different directions in both the first and the higher Brillouin zones. We also calculated the energy density distribution of these branches and found that the energy is residing mostly in the solvent. These findings imply that in the $s = 2, 3$ modes the wave is repeatedly bouncing off the spheres without penetrating into them, a result which is consistent with the large mismatch between silica and solvent.

The fourth and fifth rather flat bands in fig. 4 lie close to the single-silica-sphere eigenfrequencies associated with the $\ell = 2$ and $\ell = 3$ spherical harmonic, respectively [14]. Thus we propose that these two highest bands are essentially a coherent superposition of single-sphere eigenmodes. This is the phonon analog of the d -bands in transition metals and f -bands in rare earths, made of superposition of atomic d and f orbitals, respectively. To prove this statement, we calculated the energy density distribution of these d ($\ell = 2$) and f ($\ell = 3$) single-silica-sphere modes, and found that they are well localized inside the spheres with a weak leakage outside. The density of the energy which escapes in the solvent is small, thus weak overlap with similar modes in neighboring spheres is expected. This weak overlap is consistent with the flatness in q space and the narrowness of the corresponding frequency bands.

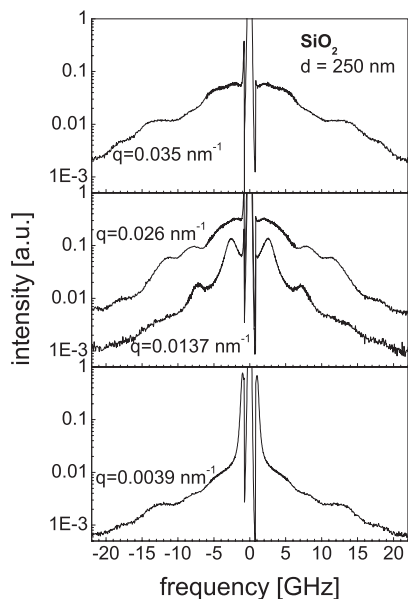


Fig. 3

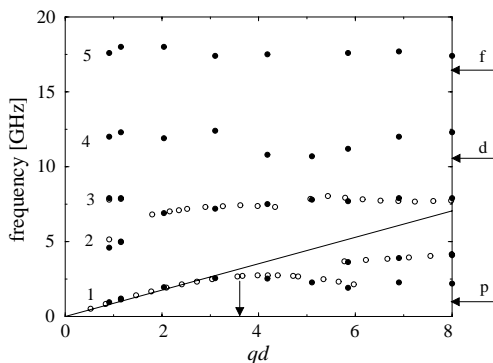


Fig. 4

Fig. 3 – Brillouin spectra obtained at four scattering wave vectors, q , for a colloidal polycrystalline suspension of silica spheres (of diameter $d \approx 250$ nm and volume fraction $\phi \approx 0.62$) in cyclohexane/decalin mixture, at 20°C . For the sake of clarity the spectrum at $q = 0.026 \text{ nm}^{-1}$ is shifted by a factor of 5.

Fig. 4 – Phonon dispersion relations for the system of fig. 3. Solid circles are the experimental data for the five observed bands, while open circles are theoretical results based on the MS method. The arrows on the vertical axis indicate the eigenfrequencies of a single silica sphere embedded in the solvent; the letters above them denote the spherical harmonic character of the corresponding eigenmodes. The arrow on the horizontal axis corresponds to the center-surface distance of the first Brillouin zone in the $[111]$ direction. The solid line fits the measured dispersion of the longitudinal phonon in the solvent.

In conclusion, we measured, for the first time, acoustic-like and optical-like phonon dispersion relations by inelastic Brillouin light scattering in *polycrystalline* colloidal suspensions. The crystallinity reveals itself by the appearance of additional modes at high q , low ω (due to the momentum transfer, $\hbar\mathbf{K}_m$, to the lattice), and at high frequency (due to the enhanced scattering strength). Four optical-like modes were observed in the crystalline silica case as opposed to one in a liquid suspension of silica particles. Also, structure at the boundary of the Brillouin zone was observed at some ω vs. q plots, indicative of the crystalline order. Significant differences, mainly in the amplitude behavior, were observed between case b) (large elastic constants contrast [7] between solvent and sphere material) and case a) (where this contrast is not large); in case a), the internal modes of each sphere mix strongly with the acoustic mode of the fluid. The data agree reasonably well with theoretical band structure results obtained by the multiple-scattering method. Simple physical explanations were proposed based partly on the vibration eigenmodes of a single sphere embedded in the solvent.

Partial financial support of the EC grants no. FMRX-CT96-0042 and HPRN-CT-2000-00017 is gratefully acknowledged.

REFERENCES

- [1] GRAHAM I. S., PICHE L. and GRANT M., *Phys. Rev. Lett.*, **64** (1990) 3135.
- [2] PAGE J. H., CHENG P., SCHRIEMER H. P., JONES I., JING X. and WEITZ D. A., *Science*, **271** (1996) 634.
- [3] LIU Z. *et al.*, *Science*, **289** (2000) 1734.
- [4] ASHCROFT N. W. and MERMIN N. D., *Solid State Physics* (Saunders College Publishing, Fort Worth, Texas) 1976.
- [5] CHENG Z., ZHU J., RUSSEL W. B. and CHAIKIN P. M., *Phys. Rev. Lett.*, **85** (2000) 1460.
- [6] HOPPENBROUWERS M. and VAN DE WATER W., *Phys. Rev. Lett.*, **80** (1998) 3871.
- [7] The relevant system parameters for the case a) are: PMMA particles: $\rho = 1180 \text{ kg/m}^3$, $c_l = 2800 \text{ m/s}$, $c_t = 1400 \text{ m/s}$ (ρ denotes the mass density and c_l (c_t) the velocity for longitudinal (transverse) waves —the c_l , c_t were obtained from the polarized and depolarized Rayleigh-Brillouin spectra of bulk PMMA glass at ambient temperature); solvent: $\rho = 926 \text{ kg/m}^3$ and $c_l = 1500 \text{ m/s}$. For the case b): solvent: $\rho = 778 \text{ kg/m}^3$, $c_l = 1270 \text{ m/s}$; silica particles: $\rho = 1830 \text{ kg/m}^3$, $c_l = 5600 \text{ m/s}$, $c_t = 3400 \text{ m/s}$. The radius of the silica particles is given in GANS B. J., PhD Thesis, Twente University, 2000.
- [8] PENCIU R. S., FYTAS G., ECONOMOU E. N., STEFFEN W. and YANNOPOULOS S. N., *Phys. Rev. Lett.*, **85** (2000) 4622.
- [9] ZHU J. *et al.*, *Nature (London)*, **387** (1997) 883.
- [10] LIU J., JE K., WEITZ D. A. and SHENG P., *Phys. Rev. Lett.*, **65** (1990) 2802; YE L., LIU J., SHENG P. and WEITZ D. A., *Phys. Rev. E*, **48** (1993) 2805.
- [11] KAFESAKI M. and ECONOMOU E. N., *Phys. Rev. B*, **60** (1999) 11993; the only approximation in this method is the truncation of the sum of spherical harmonics Y_l^m entering in the scattering amplitude of an acoustic wave by a single sphere. In fig. 2 terms up to $\ell = 4$ were kept, which guarantees the accuracy of our calculations for $\omega \lesssim 3 \text{ GHz}$.
- [12] ECONOMOU E. N. and SIGALAS M. M., *J. Acoust. Soc. Am.*, **95** (1994) 1734.
- [13] L. FLAX, G. GAUNAURD and H. ÜBERALL, *Physical Acoustics*, edited by MASON W. P., Vol. **XV** (Academic, New York) 1981.
- [14] The value of each of these eigenfrequencies is roughly proportional to c_l/d' , where c_l is the longitudinal sound velocity in the sphere material and $d' \geq d$. d' depends on the elastic constant matching between sphere material and host.